Femtosecond Visible/Visible and Visible/Mid-IR Pump−Probe Study of the Photosystem II Core Antenna Complex CP47

Marie Louise Groot,*,† Jacques Breton,‡ Luuk J. G. W. van Wilderen,† Jan P. Dekker,† and Rienk van Grondelle†

Faculty of Sciences, Vrije Universiteit, 1081 HV Amsterdam, The Netherlands, and Service de Bioénergétique, Bât. 532, CEA-Saclay, 91191 Gif-sur-Yvette, France

Received: December 22, 2003; In Final Form: March 16, 2004

CP47 is one of the two core antenna proteins of Photosystem II involved in the transfer of solar energy toward the photochemically active reaction center, the D1D2cytb559 complex. We have performed vis/vis and vis/mid-IR pump−probe experiments at room temperature as a first step in linking the energy-transfer dynamics to the arrangement of the individual chlorophylls in the CP47 complex. The chlorophylls in CP47 have very similar absorption maxima (within 20 nm of each other); therefore, few spectral changes due to energy transfer can be observed at room temperature. We used the annihilation of excitation energy as a tool to enhance the spectral changes associated with energy transfer. Energy transfer was found to occur on time scales of ∼100 fs, 1−4 ps, and 12−28 ps, and our results are consistent with the presence of two red (683-nm) pools, plus an additional red-shifted one (690 nm). From the time-resolved mid-IR spectra, it follows that these red states show a keto C═O stretching frequency at 1686 cm^{-1} and therefore are either in a polar environment or have a fairly weak hydrogen bond. For the more blue-absorbing states, we observe varying keto band positions between 1696 and 1664 cm^{-1}, and thus their hydrogen bonds strength varies between "none present" and "strong". A change in the frequency of the coordination marker mode was observed when the 690-nm state was populated, probably caused by a more planar conformation of the macrocyle of the chlorophyll responsible for the 690-nm state.

1. Introduction

The primary steps in photosynthesis of energy and electron transfer occur in green plants in two large protein complexes called Photosystem I and Photosystem II. The Photosystem II core complex consists of several individual pigment−protein complexes; these are the core antenna's CP43 and CP47 and the D1D2cytb559 reaction center. Recently, two crystal structures of PSII from cyanobacteria were reported, one at 3.8-Å[1] and one at 3.7-Å[2] resolution. In the latter structure, 17 Chl *a* molecules were found in CP47, which is one more than could be observed in the earlier structure. CP47 also binds two or three β-carotenes that were not observed in the structure.[1,2] The chlorophylls are roughly distributed in two layers near the stromal and lumenal sides of the membrane. Most of the pigments are oriented with their plane perpendicular to the membrane plane. The resolution with which these crystal structures are resolved is not high enough to recognize some of the details of the cofactors, such as the orientation of the ring plane or their binding with the protein.[23]

The CP47 and CP43 complexes serve to absorb solar photons and transfer the excited-state energy to the D1D2 reaction center. The excitation-energy trapping time in PSII cores with open RCs is about 50−100 ps;[3−5] in cores of plant PSI, with close to 200 Chls, trapping times of 50 and 120 ps have also been measured.[6] Energy transfer between groups of pigments within the isolated CP47 complex occurs on the 0.2−0.4 ps, 2−3 ps, and ∼20 ps time scales at 77 K.[7] Pools of pigments absorbing at 660, 670, 676, and 683 nm can be recognized from the (low-temperature) absorption spectrum.[7−9] An exciton calculation of the chlorophylls based on the published structure yielded results that were in agreement with the absorption spectrum and were in line with the observed energy-transfer rates.[7] From these calculations, it followed that the pigments are mainly involved in pairwise interactions. Both on the lumenal and on the stromal side a pair of Chls (35−48 and 39−42 in the Zouni nomenclature[1]) were suggested to give rise to the lowest exciton band at 683 nm. There is experimental evidence that a 690-nm state also exists in CP47, from linear dichroism,[8] hole-burning studies,[10,11] and fluorescence line-narrowing studies.[12] From a simultaneous fit of the linear dichroism and absorption spectrum, it was concluded that this state has the oscillator strength of one Chl and an ∼20% larger width than the other Chl pools (217 cm^{-1} at 77 K).[12] A weak band at 1633 cm^{-1} observed in the fluorescence line-narrowed spectrum was assigned to the Chl keto band and interpreted to be indicative of a very strong hydrogen bond with the protein, thus possibly causing the red-shifted absorption of this Chl.[12]

In the present study, we report the results of femtosecond visible pump/mid-IR probe experiments on CP47 detected in the 1600−1800-cm^{-1} region. This region mainly probes the absorption changes in the C═O stretches of the chromophore (i.e., the 9-keto and 10a-ester modes) and the protein, and a mode sensitive to the macrocycle of the chromophore. The keto and ester modes are sensitive to the polarity of the environment and the presence and strength of hydrogen bonds that the Chl may engage at these positions with the protein. Energy transfer between pigments in different environments or with different

* Corresponding author. E-mail: ML.Groot@few.vu.nl.
† Vrije Universiteit.
‡ Service de Bioénergétique.

10.1021/jp037966s CCC: $27.50
Published on Web 05/14/2004

strengths of hydrogen bonds with the protein should therefore show up as time-dependent absorption changes in the region of the 9-keto and 10a-ester bands. When a higher-resolution structure becomes available, these data may thus provide a direct link between the energy-transfer dynamics as observed in visible pump/probe experiments and the individual pigments in the CP47 complex. The experiments, performed at room temperature, are augmented by visible pump/probe experiments because only low-temperature measurements had been reported before. These experiments were performed as a function of excitation energy, causing an increasing number of ultrafast annihilation processes between a subset of the pigments, thus allowing better observation of energy-transfer events between chlorophylls.

Our results are consistent with the presence of two red (683-nm) pools plus an additional one that is further red shifted (690 nm), and the observed energy-transfer times confirm those of the 77 K experiments. We observe a variation in hydrogen bond strength between "none present" and "strong" but can find no indication of the proposed anomalously strong bond for the 690-nm pigment. We do observe a shift in the coordination marker mode for this state, which is probably due to a more planar conformation of this Chl, and we discuss the possibility that this could reflect coordination by the protein from the syn side of this Chl.[20]

2. Materials and Methods

CP47 complexes were isolated from spinach as reported before.[9] For the vis/mid-IR experiments, a D_2O buffer was used, and the samples were concentrated to ODs between 0.5 and 0.85 at 674.5 nm for a 20-μm optical path length. For the vis/vis experiments, a concentration corresponding to an optical density of 0.18 at 674.5 nm for a 20-μm path length was used. This resulted in an OD at the wavelength of excitation, 585 nm, of 0.022, so at the highest used excitation energy of 240 nJ, only 12 nJ was absorbed.

The experimental setup consisted of an integrated Ti:sapphire oscillator-regenerative amplifier laser system (Hurricane, SpectraPhysics) operating at 1 kHz and 800 nm, producing 85-fs pulses of 0.8 mJ. A portion of this 800-nm light was used to pump a noncollinear optical parametric amplifier to produce the excitation pulses with a central wavelength of 585 nm. The excitation pulses had a duration (uncompressed) of about 60 fs. They were focused with a 20-cm lens onto the sample. A second portion of the 800-nm light was used to pump an optical parametric generator and amplifier with a difference frequency generator (TOPAS, Light Conversion) to produce the mid-IR probe pulses. The probe pulses were attenuated to an intensity of about 1 nJ and were spatially overlapped with the excitation beam in the sample. The cross correlation of the visible and IR pulses was measured in GaAs to be about 180 fs.

After overlap in the sample, the mid-IR probe pulses were dispersed in a spectrograph and imaged onto a 32-element MCT detector (Infrared Associates). The signals of the detector array were amplified (Infrared Associates) and fed into 32 home-built integrate-and-hold devices that were read out every shot with a National Instruments acquisition card (PCI6031E). The polarization of the excitation pulse was set to the magic angle (54.7°) with respect to the IR probe pulses. A phase-locked chopper operating at 500 Hz was used to ensure that every other shot the sample was excited and that the change in transmission and hence optical density could be measured. To ensure a fresh spot for each laser shot, the sample was moved by a home-built Lissajous scanner.

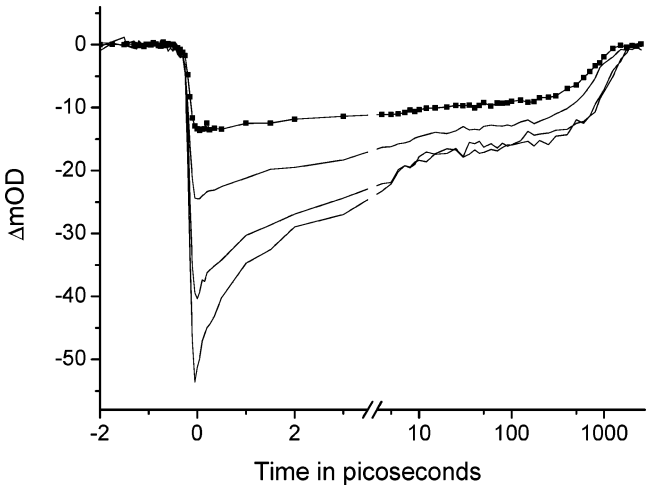

Figure 1. Time traces of CP47 at RT taken at 680 nm, upon excitation at 585 nm, as a function of incident laser power. From top to bottom 40, 80, 160, and 260 nJ; the instrument response function is 130 fs.

The vis/vis experiments were performed with the same setup, which was extended with an arm in which white light was generated in a 2-mm sapphire plate. This probe light was focused on the sample with the same lens used for the focusing of the excitation pulse, dispersed in a spectrograph, and imaged onto one of the arrays of a double, 256-element diode array (Hamamatsu S4801-256Q). The diode array was read out every shot using a 16-bit ADC (Analogue Devices) and an EDT CD-20 digital I/O board. The instrument response function in this configuration was about 130 fs. In both types of measurements, spectra at 80 different time points were collected. The data were analyzed using a global fit algorithm, which especially in the case of the mid-IR measurements, where the noise in the probe light is correlated to a large degree, led to a large decrease in the estimated standard error of the fit (75 μOD for the vis/mid-IR data set and 280 μOD for the data presented in Figure 2a.)

3. Results

Visible Pump/Visible Probe Data. Figure 1 shows time traces at 680 nm, taken at different incident laser pulse energies varying between 40 and 260 nJ, upon excitation at 585 nm. Annihilation processes clearly lead to an acceleration of the initial decay when the excitation pulse energy is increased and to the saturation of the end level for the highest excitation pulse energies. At the lowest laser pulse energy, we calculate, by dividing the areas of the absorption spectrum and of the absorption difference spectrum shortly after $t = 0$ and taking into account a 50% contribution of stimulated emission, that 2.9% of the chlorophylls are bleached. If we assume that 1 out of every 17 Chls in a CP47 complex is bleached, then this means that on average 34% of the CP47 complexes carry an excitation. That at this intensity the excitation decay kinetics are not quite annihilation-free can be seen from the fact that there is still some decay of the signal in the initial few picoseconds.

The results of a global analysis of the data taken with 40 nJ using a sequential model with increasing lifetimes are shown in Figure 2a. The initial spectrum consists of a negative band, composed of the sum of bleaching and stimulated emission, peaking at 679.5 nm. This is more or less in the middle between the room-temperature emission maximum (683 nm[9]) and the absorption maximum (674.5 nm). Excited-state absorption peaking around 650 nm is also observed. A small decay of the

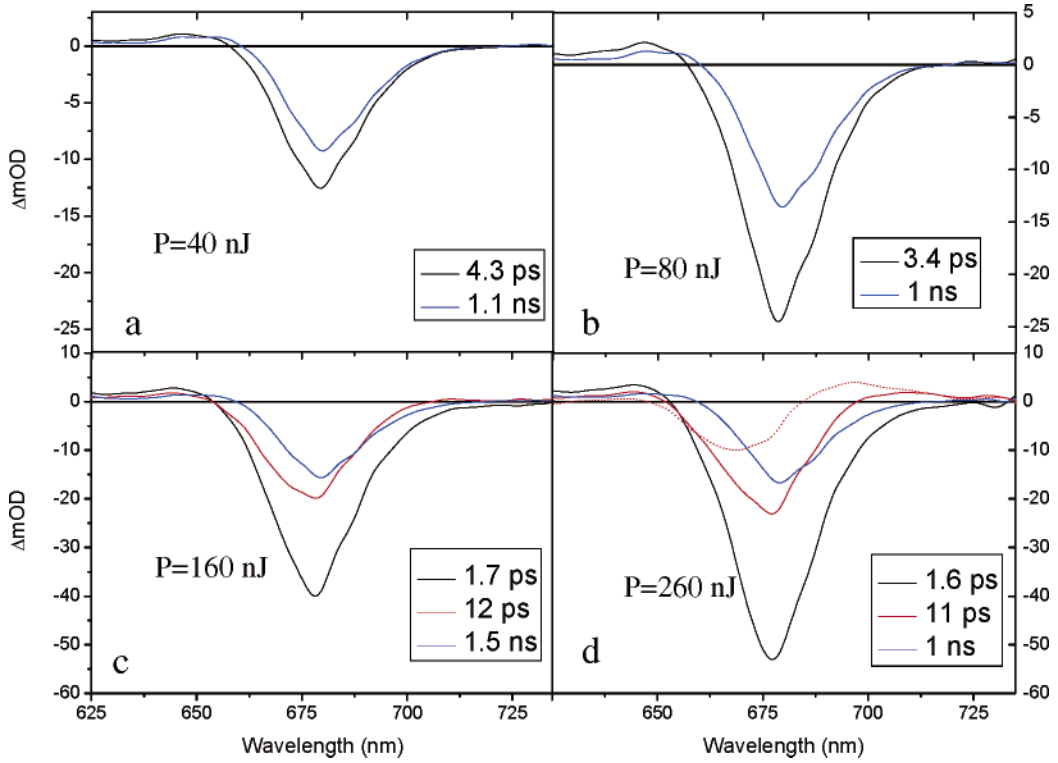

Figure 2. Species-associated difference spectra (SADS) resulting from a global analysis using a sequential model with increasing lifetimes for data sets taken with increasing excitation laser power. In d,y the double difference spectrum between the 11-ps and 1-ns lifetime spectra are also shown toenable a better comparison of the associated spectral changes (red dotted line).

initial spectrum occurs with a 4.3-ps time constant. This is followed by a slightly (0.5-nm) red-shifted spectrum with a 1-ns lifetime due to natural excited-state decay processes.

The 4.3-ps process most likely represents annihilation between slightly more blue- and slightly more red-absorbing states (i.e., the blue excitation is lost because of energy transfer, but because of the annihilation of this excitation with a previously excited red state, the corresponding red intensity is not gained). For a homogeneous complex, one would expect that with increasingly higher excitation energies this process would gain in importance, but it keeps the same spectral signature. However, we clearly see that more complicated processes start to play a role when the excitation energy is increased in CP47 (Figure 2b−d), indicating that the system should be considered to be heterogeneous, even at room temperature. The relative amplitude of the picosecond component increases, but its lifetime decreases to 1.6 ps at 260 nJ. In the two data sets with the highest laser pulse energies, the 1.7−1.6-ps component corresponds more to a decay of red intensity, instead of blue, and a component of about 12 ps appears. The latter component shows a combination of the decay of the blue part of the spectrum and an increase in the red bleaching signal and therefore describes the transfer from blue- to red-absorbing states. The double-difference spectrum has a minimum at ∼670 nm and a maximum at 696 nm (dotted lines in Figure 2d). A comparison of the different data sets reveals that all of the spectra that have an ∼1-ns lifetime have almost the same shape (Figure 3b), as expected. However, the initial spectra of the datasets with the higher excitation density clearly have more blue- and fewer red amplitudes than the corresponding spectrum of the data set with the lowest excitation density (Figure 3a). How can the initial spectra be different for different excitation densities? We can rule out the possibility that saturating excitation at 585 nm is responsible because 585 nm is a nonselective excitation wavelength. A more likely possibility is that very fast energy transfer leads to the

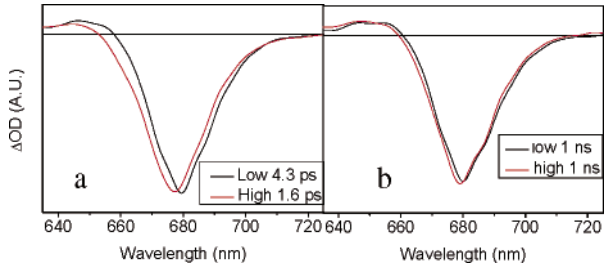

Figure 3. SADS of the first components (a) and of the longest-lived 1-ns component (b) of the high- and low-intensity data.

annihilation of slightly red-absorbing states on a <100 fs time scale (i.e., within the excitation pulse). This would further imply that the blue positive signal observed in the 40-nJ spectrum around 650 nm (which probably extends further to the red) is linked to the population of the red-absorbing states and therefore possibly represents a transition of excitonic nature. The spectra of the 1.7- and 1.6-ps components also show that on the 1.7−1.6-ps time scale, at high excitation energy, relatively more annihilation takes place on the red-absorbing Chls, leading to an even further blue-shifted difference spectrum. This must be caused by annihilation between two (or more) red states or rather two equilibrated bulk red states, whereas the presence of still excited blue states must be assumed to observe the blue shift of the difference spectrum. This process is probably mixed with the 4-ps component of Figure 2A. At least two equilibrated bulk red states must be involved in this because only then, because of the high excitation energy, it is possible to have two excitations on two red states in one complex, which then annihilate. The blue-to-red energy-transfer/annihilation component of 12 ps partially repopulates red states, illustrating that excitations were indeed still present on blue states. Considering the earlier annihilation on red states, we have to conclude that this transfer is to a third, previously unpopulated or hardly

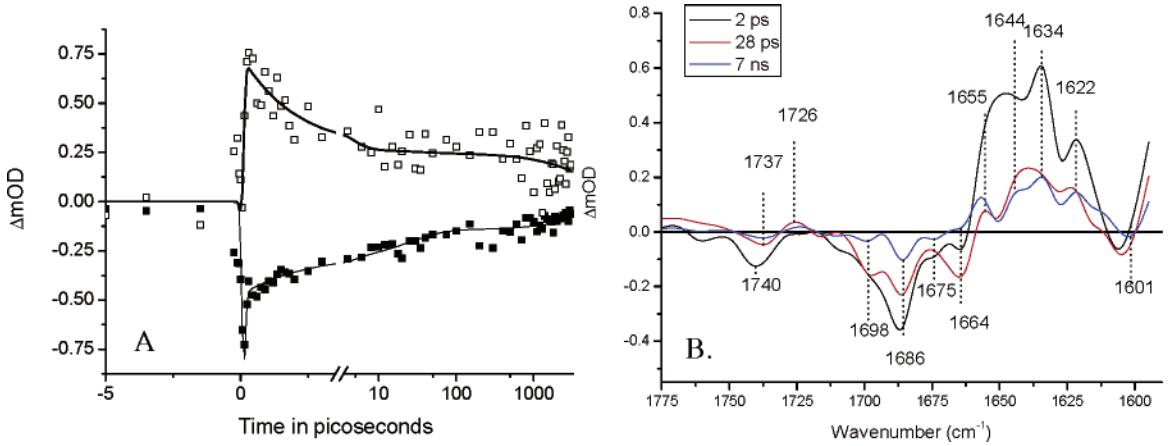

Figure 4. Pump−probe measurements in the mid-IR, excited at 585 nm. (A) Time traces detected at 1634 (top) and 1686 cm^{-1} (bottom) upon excitation at 585 nm. Note that the scale is linear up to 3 ps and logarithmic thereafter. The solid lines are a fit to the data with time constants of $t_1 = 2$ ps, $t_2 = 28$ ps, and $t_3 = 7$ ns; a very fast component that follows the instantaneous IRF is also included. Before $t = 0$, a perturbed free-induction decay signal is observed; no attempt is made to include this in the fit. (B) Species-associated difference spectra (SADS) resulting from a global analysis of the data using a sequential model with decreasing lifetimes.

populated red state. In view of the very red increase in the signal, this is most likely the 690-nm state, whereas the earlier populated red states may be identified with the 683-nm states. The reason that the energy transfer to the 690-nm state is observed in the high-excitation data and not in the low-excitation data is that a relative underpopulation of red states is achieved by the annihilation. In the low-excitation-energy spectra, ∼12 ps transfer to the 690-nm state also occurs, but the spectral change accompanying the change in equilibration when the 690-nm state becomes populated is apparently very small (because it corresponds in a first approximation to the difference between populating a single 683-nm or a single 690-nm state).

In conclusion, we have observed blue-to-red energy transfer occurring in about 4 ps and blue-to-red (690-nm) energy transfer with a rate accelerated by annihilation in about 12 ps, and we deduce from the intensity-dependent spectra that fast, ∼100-fs energy transfer to (or between, but see next argument) red states occurs and that two of the red states are in contact with each other on an ∼1−2-ps time scale. These findings are in good agreement with the 77 K work of De Weerd et al.,[7] who found in streak camera experiments, performed at low excitation energy, time constants of 4 and 28 ps and in pump−probe experiments, probably performed with higher excitation energy, downhill energy transfer in 1.9 and 18 ps as well as a 0.2−0.3-ps process. The 17-ps component they assigned to the partial population of a red 690-nm state from a 683-nm state. The fact that we observe that transfer occurs from more blue states, as can be seen from the minimum in the double-difference spectrum of Figure 2d, is probably the consequence of the more extensive equilibration over the different states at room temperature.

Visible Pump/Mid-IR Probe Data. Figure 4 shows two time traces and the species-associated spectra that result from a global analysis of the data probed between 1775 and 1580 cm^{-1}. Three kinetic components are needed to fit the data; 2 ps, 28 ps, and 7 ns. These time constants are in good agreement with the data discussed above. In all components, we see net decay, indicating that annihilation takes place, and we are most likely in the regime comparable to that of the 160- and 260-nJ visible experiments.

The 2-ps spectrum shows negative bands at 1740, 1686, 1664, and 1606 cm^{-1} and a shoulder at 1698 cm^{-1}. Negative bands in the 1700−1640-cm^{-1} region can be assigned to the 9-keto modes of different Chl molecules in the ground state. The free keto band of Chl *a* in THF is observed at 1695−1697 cm^{-1}.[13−16] This mode may downshift more than 10 cm^{-1} depending on the dielectric properties of the environment,[17] whereas increasing hydrogen bond strength also shifts this mode to even lower frequency. Judging from its high frequency, the 1698-cm^{-1} mode arises from a (set of) Chl molecule(s) in an apolar environment, whereas the 1664-cm^{-1} mode is at such low frequency that the keto group of this Chl molecule is most likely involved in a strong hydrogen bond interaction. The moderate 10-cm^{-1} downshift of the 1686-cm^{-1} mode may be caused either by a Chl having either a free keto group in a polar environment or a weak hydrogen bond interaction.

It can be seen that in the excited state the 9-keto modes downshift to the 1650−1610-cm^{-1} frequency range. For comparison, the keto of Chl *a* in the triplet state shifts from 1697 to 1666 cm^{-1} in THF.[15,16] In Raman experiments on CP47, only three populations of Chls were observed with C═O frequencies at 1670, 1688, and 1701 cm^{-1},[18] which correspond well with the frequencies we find here. Because the CP47 protein contains 17 pigments, we conclude that more than one pigment contributes to the bands we observe here. In the Discussion section, where the time behavior is discussed in more detail and in relation to the visible pump−probe experiments, we will elaborate on this point.

The 28-ps spectrum shows some additional structure: a bandshift from 1737 to 1726 cm^{-1} due to the C═O stretch of a 10a-ester is observed; the band at 1698 cm^{-1} has developed more clearly; and the 1664-cm^{-1} band has increased significantly. The increase of the 1664-cm^{-1} band is remarkable because an overall decay of the signal is observed in the vis/vis experiments. We suggest that this apparent increase in bleaching is caused by the disappearance of a positive overlapping keto−excited state absorption. Indeed, in the 7-ns spectrum, where apparently the 1664-cm^{-1} band has disappeared, the excited-state contribution from other keto groups still causes a net positive signal at 1664 cm^{-1}, even when its signal is much smaller. The overlapping excited-state contribution makes it impossible to follow its population change occurring with the 2-ps time constant. The 1606-cm^{-1} mode is due to a Chl skeletal vibration. This mode is sensitive to the coordination number; a 5-coordinated Chl typically is at 1609−1607 cm^{-1} in THF, and a 6-coordinated molecule is at 1597 cm^{-1}.[21] Possibly the position

of this band has downshifted somewhat due to the positive contributions of the keto-excited state on the high-frequency side. With the decay of the 28-ps spectrum, this band shifts further to 1601 cm^{-1}, suggesting more localization of the excitation on a Chl with a perturbed coordination marker mode. Also, the negative band at 1664 cm^{-1} disappears.

To summarize, first the excitation seems to be mainly localized on a (set of) Chls having a keto group in a polar environment or with a relatively weak hydrogen bond at 1686 cm^{-1} and on a (set of) Chls with a strong hydrogen bond at 1664 cm^{-1}. Then, in ~2 ps, the energy annihilates, and a net higher population of (a set of) Chls with no hydrogen bond in an apolar environment (keto at 1698 cm^{-1}) is achieved; the population change of the 1664-cm^{-1} mode is unknown. Finally, in ~20 ps, population disappears from mainly the 1664- and 1698-cm^{-1} Chl(s). A shift to 1601 cm^{-1} of the coordination marker is observed in the last spectrum.

4. Discussion

Combining the results of the vis/vis and vis/mid-IR experiments, we conclude that the initially excited population is distributed over Chls with a varying dielectric environment and hydrogen bond strength, as judged from the position of the initially bleached keto bands at 1698 and 1686 cm^{-1} and the band at 1664 cm^{-1} being inferred to be populated also at early delay times. Annihilation on red states in ~1−2 ps leads to, apart from overall less population in these states, a relative decrease in population of the 1686-cm^{-1} mode. The change in population of the 1664-cm^{-1} mode cannot be estimated with this time constant. Repopulation of the red states, in particular the 690-nm state, and depopulation of the blue states leads to a relative increase of the 1686-cm^{-1} mode and decrease of the 1664- and 1698-cm^{-1} modes. We conclude that the more blue-absorbing pigments have no hydrogen bond and some have a relatively strong one. We see no convincing evidence for a 1633-cm^{-1} mode, although we do note that it would overlap with the excited-state keto bands of the other Chls and that it does show time behavior consistent with that of the 690-nm state. We suggest that red states, any or all of the 683-nm states and possibly also the 690-nm state, are in a polar environment or have a fairly weak hydrogen bond, resulting in keto bands at 1686 cm^{-1}.

The question is whether this is enough to explain the red-shifted absorption of the 690-nm pigment. We do observe a downshift of the coordination marker mode upon the preferential population of the 690-nm Chl, suggesting a more planar conformation of its macrocycle. We consider it unlikely that the marker has downshifted because the 690-nm Chl in CP47 is six-coordinated because the work of Shen and Vermaas[22] shows that the low-temperature emission at 695 nm (coming from the 690-nm state) disappears upon the mutation of a single His residue to Tyr in the hydrophobic region of CP47 and the replacement of a Chl by a Pheo is observed. A somewhat smaller downshift of the marker mode, and of other modes sensitive to the macrocycle conformation, has been observed in Raman spectra of BChls in a few other complexes. Those were interpreted as being due to BChls with a disturbed, more planar macrocycle.[19] A suggestion of what may cause the more planar conformation of the macrocycle, or at least the shift of the marker mode in a direction that would suggest this, comes from a recent study of the coordination pattern and conformation of the macrocycle of the chlorophylls in Photosystem I,[20] made possible by the high-resolution structure (2.5 Å) available for that complex.[7] It was found that the chlorophyll molecules preferentially bind to the protein from one side (anti) and much less from the other (syn) side, the ratio being 82:14. No six-coordinated Chls were found. In FMO, the only other antenna complex resolved with enough resolution to produce a ratio of 5:2 for anti and syn ligation was found. In light of this work, we should consider the possibility that the conformation marker mode is actually equally sensitive to the direction of coordination by a single ligand due to the change in the permanent dipole moment that occurs upon syn ligation.[20] However, this issue can be resolved only by X-ray structures at higher resolution and additional studies of the effect of the macrocycle conformation and coordination direction on the marker mode frequency. At present, we suggest the possibility that in CP47 a perturbed macrocycle conformation leads to a red shift of the electronic absorption.

5. Conclusions

We have shown that with femtosecond mid-infrared spectroscopy energy transfer between pigments with different hydrogen bond strength can be observed. Especially in the case of CP47, where at room temperature the individual pigments have very similar electronic absorption spectra, this technique adds valuable knowledge to the flow of energy transfer within the complex. We hope that these data can be combined with a high-resolution crystal structure to obtain a good understanding of the structure−dynamics relationship in CP47.

Acknowledgment. This research was supported by the Netherlands Organization for Scientific Research via the Dutch Foundation for Earth and Life Sciences (investment grant no. 834.01.002) and by the European Union, Human Resources and Mobility Activity, contract no. MRTN-CT-2003-505069. M.-L.G. is grateful to the NWO-ALW for providing financial support with a long-term Vidi fellowship.

References and Notes

(1) Zouni, A.; Witt, H. T.; Kern, J.; Fromme, P.; Krauss, N.; Saenger, W.; Orth, P. *Nature* **2001**, *409*, 739−743.

(2) Kamiya, N.; Shen, J.-R. *Proc. Natl. Acad. Sci. U.S.A.* **2003**, *100*, 98−103.

(3) Schatz, G. H.; Brock, H.; Holzwarth, A. R. *Biophys. J.* **1988**, *54*, 397−405.

(4) Van Grondelle, R.; Dekker: J. P.; Gillbro, T.; Sundstrom, V. *Biochim. Biophys. Acta* **1994**, *1187*, 1−65.

(5) Barter, L. M. C.; Bianchietti, M.; Jeans, C.; Schilstra, M. J.; Hankamer, B.; Diner, B. A.; Barber, J.; Durrant, J. R.; Klug, D. R. *Biochemistry* **2001**, *40*, 4026−4034.

(6) Ihalainen, J. A.; Jensen, P. E.; Haldrup, A.; Van Stokkum, I. H. M.; Van Grondelle, R.; Scheller, H. V.; Dekker, J. P. *Biophys. J.* **2002**, *83*, 2190−2201.

(7) De Weerd, F. L.; Van Stokkum, I. H. M.; Van Amerongen, H.; Dekker, J. P.; Van Grondelle, R. *Biophys. J.* **2002**, *82*, 1586−1597.

(8) Van Dorsen, R. J.; Breton, J.; Plijter, J. J.; Satoh, K.; Van Gorkom, H. J.; Amesz, J. *Biochim. Biophys. Acta* **1987**, *893*, 267−274.

(9) Groot, M. L.; Peterman, E. J. G.; Van Stokkum, I. H. M.; Dekker: J. P.; Van Grondelle, R. *Biophys. J.* **1995**, *68*, 281−290.

(10) Chang, H. C.; Jankowiak, R.; Yocum, C. F.; Picorel, R.; Alfonso, M.; Seibert, M.; Small, G. J. *J. Phys. Chem.* **1994**, *98*, 7717−7724.

(11) Den Hartog, F. T. H.; Dekker: J. P.; Van Grondelle, R.; Volker, S. *J. Phys. Chem. B* **1998**, *102*, 11007−11016.

(12) De Weerd, F. L.; Palacios, M. A.; Andrizhiyevskaya, E. G.; Dekker, J. P.; Van Grondelle, R. *Biochemistry* **2002**, *41*, 15224−15233.

(13) Feiler, U.; Mattioli, T. A.; Katheder, I.; Scheer, H.; Lutz, M.; Robert, B. *J. Raman Spectrosc.* **1994**, *25*, 365−370.

(14) Pascal, A. A.; Caron, L.; Rousseau, B.; Lapouge, K.; Duval, J.-C.; Robert, B. *Biochemistry* **1998**, *37*, 2450−2457.

(15) Breton, J.; Nabedryk, E. In *Fifth International Conference on the Spectroscopy of Biological Molecules*; Theophanides, T. et al., Eds.; Kluwer Academic: Dordrecht, The Netherlands, 1993; pp 309−310.
(16) Noguchi, T.; Tomo, T.; Inoue, Y. *Biochemistry* **1993**, *32*, 7186−7195.
(17) Lapouge, K.; Naveke, A.; Sturgis, J. N.; Hartwich, G.; Renaud, D.; Simonin, I.; Lutz, M.; Scheer, H.; Robert, B. *J. Raman Spectrosc.* **1998**, *29*, 977−981.
(18) De Paula, J. C.; Liefshitz, A.; Hinsley, S.; Lin, W.; Chopra, V.; Long, K.; Williams, S. A.; Betts, S.; Yocum, C. F. *Biochemistry* **1994**, *33*, 1455−1466.
(19) Lapouge, K.; Naveke, A.; Gall, A.; Ivancich, A.; Segui, J.; Scheer, H., Sturgis, J. N.; Mattioli, T. A.; Robert, B. *Biochemistry* **1999**, *38*, 11115−11121.
(20) Balaban, T. S.; Fromme, P.; Holzwarth, A. R.; Krauss, N.; Prokhorenko, V. I. *Biochim. Biophys. Acta* **2002**, *1556*, 197−207.
(21) Fujiwara, M.; Tasumi, M. *J. Phys. Chem.* **1986**, *90*, 250−255.
(22) Shen, G. Z.; Vermaas, W. F. J. *Biochemistry* **1994**, *33*, 7379−7388.
(23) After the submission of this article, a higher-resolution (i.e., 3.5-Å) structure of PSII appeared **(**Ferreira, K. N.; Iverson, T. M.; Maghlaoui, K.; Barber, J.; Iwata, S. *Science*, published online Feb 5, 2004).